The Cryosphere Discuss., 4, 77–119, 2010
www.the-cryosphere-discuss.net/4/77/2010/

The Cryosphere Discussions

This discussion paper is/has been under review for the journal The Cryosphere (TC).
Please refer to the corresponding final paper in TC if available.

Applicability of time-lapse refraction seismic tomography for the detection of ground ice degradation

C. Hilbich

Institute for Geography, University of Jena, Germany

Institute for Geography, University of Zurich, Switzerland

Received: 22 December 2009 – Accepted: 4 January 2010 – Published: 27 January 2010

Correspondence to: C. Hilbich (chilbich@geo.uzh.ch)

Published by Copernicus Publications on behalf of the European Geosciences Union.

Abstract

The ice content of the subsurface is a major factor controlling the natural hazard potential of permafrost degradation in alpine terrain. Monitoring of changes in ground ice content is therefore similarly important as temperature monitoring in mountain permafrost. Although electrical resistivity tomography monitoring (ERTM) has proved to be a valuable tool for the observation of ground ice degradation, results are often ambiguous or contaminated by inversion artefacts. In theory, the P-wave velocity of seismic waves is similarly sensitive to phase changes between unfrozen water and ice. Provided that the general conditions (lithology, stratigraphy, state of weathering, pore space) remain unchanged over the observation period, temporal changes in the observed travel times of repeated seismic measurements should indicate changes in the ice and water content within the pores and fractures of the subsurface material. In this paper, the applicability of refraction seismic tomography monitoring (RSTM) as an independent and complementary method to ERTM is analysed for two test sites in the Swiss Alps. The development and validation of an appropriate RSTM approach involves a) the comparison of time-lapse seismograms and analysis of reproducibility of the seismic signal, b) the analysis of time-lapse travel time curves with respect to shifts in travel times and changes in P-wave velocities, and c) the comparison of inverted tomograms including the quantification of velocity changes. Results show a high potential of the RSTM approach concerning the detection of altered subsurface conditions caused by freezing and thawing processes. For velocity changes on the order of 3000 m/s even an unambiguous identification of significant ground ice loss is possible.

1 Motivation

Monitoring of permafrost in polar and mountainous regions becomes more and more important in the context of ongoing global warming. A key parameter concerning slope stability analyses and permafrost modelling purposes is the ice content of the subsur-

TCD

4, 77–119, 2010

face and its temporal evolution (Harris et al., 2009). Thermal monitoring in boreholes is a common and widespread method to observe permafrost evolution (e.g., Harris and Isaksen, 2008; PERMOS, 2009), but does only provide indirect insights into ice content changes. Many geophysical methods are more sensitive to changes in water content than to temperature variations, and in particular to phase transitions between frozen and unfrozen water. Fortier et al. (1994) showed that variations of apparent resistivity with time can be used to predict unfrozen water and ice contents of the frozen ground. Recent studies on the applicability of electrical resistivity tomography monitoring (ERTM) proved the high sensitivity of ERT to spatio-temporal changes in the subsurface ice and water contents (Hauck, 2002; Hilbich et al., 2008; Kneisel et al., 2008; Hilbich, 2009).

Apart from ERTM, repeated refraction seismic measurements theoretically have a considerable potential to observe permafrost evolution, since the seismic P-wave velocity (v_p) is highly sensitive to variations in the ice or water content (by changes in v_p between frozen and unfrozen water of up to 2000 m/s). Due to its complementary nature, seismic refraction is often considered to be a valuable additional method to verify subsurface structures identified by ERT (e.g., Hauck and Vonder Mühll, 2003; Kneisel et al., 2008). Seismic refraction is generally capable of discriminating unfrozen and frozen sediments or massive ice, and is thus a common method to determine active layer thickness. However, the largely overlapping ranges of P-wave velocities for ice and bedrock (both frozen and unfrozen) make a differentiation of stratigraphic details in bedrock and/or below the permafrost table (e.g. in rock glaciers or talus slopes) often difficult. Together with the comparatively high measurement and processing efforts, this may be a reason why refraction seismic surveys are less popular in permafrost research than e.g. ERT or GPR measurements. Nevertheless, numerous studies successfully applied refraction seismic surveys in permafrost terrain (e.g., Röthlisberger, 1972; Harris and Cook, 1986; Vonder Mühll, 1993; Musil et al., 2002; Hauck et al., 2004; Ikeda, 2006; Hausmann et al., 2007; Maurer and Hauck, 2007), and main advantages of the method, compared to ERT surveys, are e.g. the much higher depth

resolution (Lanz et al., 1998), the potential to exactly localise sharp layer boundaries, the less challenging coupling of the sensors in blocky terrain, or the applicability in terrain with electrically conductive infrastructure contaminating the resistivity signal.

Provided that the general conditions (lithology, stratigraphy, state of weathering, pore space) remain unchanged over the observation period, changes in the ice and water content within the pores and fractures of the subsurface material should similarly or even better be detectable by repeated measurements than for ERT. Despite the ambiguities involved in a qualitative stratigraphic interpretation (due to overlapping velocity ranges of different materials), even comparatively small temporal changes in P-wave velocities may indicate zones with significant ground ice content changes due to seasonal variations or long-term climate change.

According to the theoretical suitability of a refraction seismic tomography monitoring (RSTM) approach to permafrost related research, the potential of an independent and complementary monitoring method to determine relative ice (and water) content changes in the subsurface will be evaluated in this paper.

2 Theory and approach

Apart from a vast research related to *reflection* seismic monitoring of deep reservoirs in exploration geophysics (see e.g., Vesnaver et al., 2003; King, 2005), similar efforts to investigate the potential of a *refraction* seismic monitoring approach for the observation of shallow targets have not been reported so far.

In exploration geophysics the detection of changes in reservoir velocity and compaction (due to oil production) is preferably done using reflection seismics due to their high resolution potential. However, reflection data rarely provide information on the very shallow parts of an unconsolidated sedimentary section, as seismic reflections from the upper 5–15 m of the Earth are usually overwhelmed by contaminating effects from different coincident-arriving waves. They are more affected by scattering effects in highly heterogeneous material with shallow low velocity layers than seismic refrac-

tions (Lanz et al., 1998), which is the typical situation for mountain permafrost sites. According to Lanz et al. (1998) and Musil et al. (2002) refraction seismic tomography is therefore more appropriate for exploring the upper 50 m of the subsurface.

For deep reservoirs, a first approach in using time-lapse refraction seismics was introduced by Landrø et al. (2004) for the estimation of reservoir velocity changes. It is based on the fact, that a velocity change in a reservoir (due to oil production) by only 1% will change the critical angle of refraction and thus the critical offset for refracted waves, i.e. their first appearance at the surface. For oil reservoirs located at depths of >1000 m this change in critical offset amounts to several tens of meters (Landrø et al., 2004). For shallow targets the corresponding difference in critical offsets would be reduced to a few centimetres to decimetres, making this approach inappropriate for the monitoring of mountain permafrost evolution. Concerning shallow applications, no operationally applicable time-lapse refraction seismic approach was published so far, neither for permafrost, nor for other fields of interest.

The presence of ice in the pore spaces of sediments can cause large increases in seismic velocity compared to the velocity when the interstitial water is unfrozen (Timur, 1968). Since ice is much stiffer than water, the wave speed is a strongly increasing function of the ice-to-water ratio. However, rock is much stiffer than either ice or water, therefore the wave speed is also a decreasing function of the porosity Φ (Zimmerman and King, 1986). Following Wyllie et al. (1956), who related the bulk seismic velocity v to the porosity Φ (and the interstitial water) of a medium, Timur (1968) proposed a three-phase time-average equation, which accounts for an ice-liquid-rock matrix under permafrost conditions:

$$\frac{1}{v} = \frac{(1-f_i)\Phi}{v_w} + \frac{f_i\Phi}{v_i} + \frac{1-\Phi}{v_r} \quad (1)$$

with f_i being the fraction of the pore space filled with ice, and v_i, v_r, and v_w the velocities of ice, solid rock, and the interstitial pore water. This equation simply relates the bulk velocity of a medium to the respective fractions of the components of the matrix and

their seismic velocities. To account for all components of a subsurface material, theoretically, Eq. (1) can be extended by a term relating the fraction of the air-filled pore space f_a to the seismic velocity of air v_a (Hauck et al., 2008):

$$\frac{1}{v} = \frac{f_w}{v_w} + \frac{f_r}{v_r} + \frac{f_i}{v_i} + \frac{f_a}{v_a} \quad (2)$$

Analysing the relation of the compressional velocity and the gaseous (air), liquid (water), and two solid (rock/soil, ice) components of the subsurface as a function of temperature reveals that the bulk velocity of a medium is generally higher under frozen compared to that of unfrozen conditions. Relating the temperature dependence to time, thawing causes a decreasing and freezing an increasing velocity, respectively. The velocity change depends mainly on the porosity and the initial saturation, and is thus more pronounced for unconsolidated coarse-grained sediments than for consolidated rocks (Scott et al., 1990).

These relations can be used to observe the permafrost evolution via repeated seismic measurements. The principle of a time-lapse refraction seismic approach is exemplarily illustrated in Fig. 1 for a coarse grained material with water- and/or air filled voids. From a permafrost degradation point of view, not only a degradation from above (Fig. 1b) but also an overall warming of the permafrost may be detected by increasing amounts of unfrozen water or air (as a consequence of draining), as roughly indicated in Fig. 1c. Necessary conditions to reliably detect subsurface changes via refraction seismic monitoring include a constant source-receiver-geometry between subsequent measurements and an amount of P-wave velocity change that is well above the noise level.

The measured time-lapse seismic data can then be successively processed and analysed using standard methods for tomographic inversion of seismic data (e.g., Sandmeier, 2008). The development and validation of an appropriate RSTM approach involves an evaluation of a hierarchy of methods:

a) The comparison of time-lapse seismograms and analysis of reproducibility of the

seismic signal.

b) The analysis of time-lapse travel time curves with respect to resolving possible shifts in travel times and changes in P-wave velocities.

c) The comparison of inverted tomograms including the quantification of spatio-temporal velocity changes (time-lapse tomography).

In the following, the potential and limitations for the application of time-lapse refraction seismic in high mountain permafrost environments will be analysed based on monitoring data from two different permafrost sites.

3 Site description and data sets

To evaluate the RSTM approach repeated refraction seismic measurements were carried out at two different permafrost test sites for intervals of roughly 1.5 months, respectively, in the summer season of 2008. The test sites comprise a) the ventilated Lapires talus slope in the Valais, and b) the north oriented slope of the Schilthorn summit in the Bernese Alps (see Fig. 2).

The Lapires site is a vast concave talus slope, oriented in NE direction, which extends over more than 500 m width between 2350 and 2700 m altitude. Lithology consists of metamorphic clasts (mainly gneiss) (Vonder Mühll et al., 2007). Excavations for the installation of two cable car pylons in summer 1998 exposed sediments more or less saturated with ice (Lambiel, 1999; Delaloye et al., 2001). The frozen zone starts at around 4 m depth and has a maximum thickness of about 20 m. The thermal regime can be described as temperate (warm) permafrost. According to Delaloye and Lambiel (2005) the existence of permafrost at this site is (at least partly) due to an internal air circulation that contributes to the cooling of the talus slope. RST measurements were conducted along a permanent ERT profile (described in Hilbich, 2009) in horizontal direction traversing a pylon and a borehole. The ERT data acquired in parallel to the

RSTM measurements will be shown for comparison in Sect. 5.3. A detailed discussion of the ERTM approach and the data can be found in Hilbich (2009).

The Schilthorn massif with the summit at 2970 m altitude is located close to Mürren at the transition between the Prealps in the north and the principal chain of the Bernese Alps in the southeast. It consists of metamorphic sedimentary rocks dominated by deeply weathered dark limestone schists with a fine-grained debris cover (up to several meters thick) around the summit area (Imhof et al., 2000; Vonder Mühll et al., 2007). The presence of permafrost was first observed in 1965 during the construction of the summit station (Imhof et al., 2000) and further proved by three boreholes drilled into the north facing slope approximately 60 m below the ridge to monitor thermal permafrost evolution (Harris et al., 2003). The permafrost base was not reached by the 100 m deep boreholes. Permafrost conditions at Schilthorn are rather warm, and according to the material exposed during drilling, the ice content seems to be very low (personal communication D. Vonder Mühll). The average maximum active layer thickness is with about 5 m relatively high. RST measurements were conducted along a permanent ERT profile (described in Hilbich et al., 2008) in horizontal direction within the north facing slope, traversing the boreholes. As for the Lapires site, corresponding ERT measurements will be shown for comparison in Sect. 5.3.

This study is focused on a detailed analysis of data sets acquired in parallel at both sites in July and August 2008. The first measurement date roughly represents the end of the snowmelt season, when the active layer starts thawing, whereas the second date corresponds to an already well developed thawed active layer. Because of its pronounced changes, this seasonal interval is well suited to evaluate the general applicability of RSTM. To account for the potential to detect not only seasonal but also annual differences, a further data set from Schilthorn after one year (August 2009) will be discussed at the end of the paper. At both sites borehole temperatures are available for validation of the geophysical data.

4 Data acquisition and processing

To guarantee identical geophone positions for successive measurements, in all cases where large blocks were available the geophones were fixed via screws to the blocks, which also assures an optimal coupling to the ground. In cases of fine-grained unconsolidated surface material the geophones were fixed to the ground via spikes and positions of geophones and shot points were marked to enable relocation for later measurements.

The seismic signal was generated by a sledge hammer striking a steel plate or firm boulders where available. Signal stacking of minimum 10–20 stacks was necessary to achieve an adequate signal-to-noise ratio. Depending on the overall length of the profiles up to 40 stacks were carried out for the far shots. Shot points were placed at the midpoint between each pair of geophones to guarantee a high spatial resolution for the tomographic inversion (Maurer and Hauck, 2007). Table 1 summarises the details of data acquisition and the respective active layer depths in the nearby boreholes at the dates of measurement.

Data processing (first arrival picking, travel time analysis, tomographic inversion) was done using the software REFLEXW (Sandmeier, 2008). The reconstruction of the 2-D velocity pattern of the subsurface is based on the automatic iterative adaptation of synthetic travel times (calculated by forward modelling) to observed travel times using the so-called SIRT (Simultaneous Iterative Reconstruction Technique) inversion algorithm (Sandmeier, 2008). A starting model has to be defined that consists ideally of a gradient model with increasing velocities with depth reflecting the gross structure of the study area. Starting from this initial model synthetic travel times are calculated by forward modelling, which are then compared to the observed data. Based on the travel time residuals the initial model is adapted and synthetic traveltimes are again calculated for the new model. This iterative process stops as soon as distinct stopping criteria are fulfilled, e.g. if the relative change between subsequent iterations is smaller than a predefined value, or a maximum number of iterations is reached. The same

settings were used for all inversions.

5 Results

In the following, the two data sets acquired during a time span of 40 days (at Lapires) and 47 days (at Schilthorn) in summer 2008 will be analysed.

5.1 Analysis of seismograms

5.1.1 Lapires

Figure 3a exemplarily illustrates a detailed view of an unfiltered part of a selected seismogram with the traces for two measurement dates: 10 July (grey) and 18 August 2008 (red). Striking features of this seismogram are a) the very similar waveforms of corresponding traces from both dates pointing to a high reproducibility of the seismic signal for subsequent measurements, and b) the generally earlier arrival times of the waves in July compared to those from August with a time shift of about 1–3 ms between the two dates (highlighted in Fig. 3a).

5.1.2 Schilthorn

A detailed view of an unfiltered part of a selected time-lapse seismogram from Schilthorn is shown in Fig. 3b with the traces for the dates: 11 July (grey) and 26 August 2008 (red). Compared to Fig. 3a the time shift of first arrivals between July and August is with about 3–8 ms considerably more pronounced. The waveforms of coincident traces from both dates show less correspondence, which are supposed to be caused by considerably longer travel paths of the waves due to a lowered refractor depth in August and a correspondingly altered seismic signal.

5.2 Analysis of travel time curves

5.2.1 Lapires

First arrivals were picked manually for all 24 seismograms corresponding to 24 shot points. For data sets from coarse blocky sites with considerable surface roughness the identification of the first arrivals is sometimes complicated by their irregular distribution. In this context the high reproducibility of the signal was therefore utilised to increase the confidence in the identification of the first arrivals by jointly analysing both data sets for first arrival picking (as illustrated in Fig. 3). Especially at far distances from the shot points, where the signal-to-noise ratio usually decreases, this "constrained picking" considerably improved the accuracy in identifying the first breaks.

All picked first arrivals are displayed as combined travel time curves in Fig. 4. The superposition of corresponding pairs of travel time curves (grey July, red August) allows the analysis of differences between the two dates (hereby, the complete travel time data set was divided into three different plots for better visibility). The combined travel time curves can provide information on a) changes in the slope of the travel time curves indicating altered ice and water contents of certain layers, and/or b) time shifts in travel times indicating a shift in the depth of a refractor (e.g. the seasonally varying interface between frozen and unfrozen conditions).

The consistent pattern of these curves for both dates again confirms the general reproducibility of the overall pattern of first arrivals. Note, that some missing picks for large source-receiver distances (due to an uncertain identification of some first breaks as a consequence of low signal-to-noise ratios) cause differences in total travel times for corresponding forward and reverse traverses.

Main parts of the travel time curves (indicated in Fig. 4) comprise homogeneously low velocities in the uppermost layer of the whole profile (zone A), only slightly increased velocities for later arrivals in zone B, and a clear refractor characterised by a sharp velocity increase in zone C.

Regarding the temporal evolution of travel times, the first arrivals for the data set from

July are slightly earlier than for the second measurement in August. Important features of the time-lapse travel time plot are:

a) small or even absent travel time differences in zones A and B,

b) significant deviations from the mean displacement for some shots in zone C (e.g. at 1044, 1124, 1172, and 1180 m horizontal distance), which may indicate a change in the form of the refractor (according to Reynolds, 1997), i.e. locally pronounced changes in the refractor depth,

c) differences between both dates are generally characterised by time shifts of the travel time curves rather than by clear changes in the velocities of certain layers.

Plotting the travel times against the absolute offset between source and receiver (after Hausmann et al., 2007) reveals a clustering according to the dominant layers of the subsurface that allows a rough estimation of the mean velocities of the respective materials (indicated in Fig. 5a). As the Lapires site exhibits pronounced lateral differences the common offset plot shows two separate branches with the lowermost branch caused by a delayed arrival (longer travel time) of waves traversing zones B and C instead of only C (uppermost branch). The mean velocity close to the surface is relatively low (ca. 650 m/s) and corresponds to the unconsolidated coarse blocky layer of the talus slope. Almost no increase in velocity is observed within zone B (mean velocity about 780 m/s), indicating that no clear refractor is detectable within the investigation depth of the survey geometry, thus strongly restricting the information on the left side of the profile. The mean velocity of the only significant refractor observed amounts to 3500 m/s and is indicative for ground ice (Röthlisberger, 1972).

Figure 5b shows the observed travel time differences between July and August plotted against the absolute source-receiver offset. The majority of travel time differences between August and July are positive indicating an increase in travel time. The dependence of the travel time differences from the shot location is small for all offsets greater 20 m (Fig. 5b), meaning that the travel time shifts are caused close to the surface and

only minor velocity changes (corresponding to ice content changes) are expected at greater depth.

5.2.2 Schilthorn

The corresponding travel time curves for the Schilthorn data set are shown in Fig. 6. Comparing the travel time curves for both dates emphasises the pronounced difference between July and August observed in the seismogram of Fig. 3b. The low velocity surface layer has considerably increased in August making a direct comparison of corresponding travel time curves for subsequent measurements difficult (or not useful). However, common characteristics of the data sets comprise a basically constant velocity of the surface layer (zone A), and the irregular pattern of the travel times in zone B indicating a pronounced topography of the refractor. Features in the travel time pattern which disappear between July and August (zone C) may be related to ice occurrences, while features consistent over time (zone D) may point to structural information of the bedrock topography.

A rough interpretation of the observed features includes a significant thickening of the low velocity surface layer, i.e. a lowering of the refractor. This is a consequence of thawing processes allowing insights into a more differentiated structural pattern in August which was "hidden" during the frozen conditions in July.

The common offset plot of the travel times in Fig. 7 appears very similar for both dates and basically shows two layers with average velocities of about 590 m/s for the surface layer and 3500 m/s at greater depth. The velocity of the anomalous zone D in Fig. 6 cannot be determined from Fig. 7. As the travel time differences are much higher than for Lapires, a systematic analysis of the travel times is only of limited use and the analysis will focus on the inverted tomograms.

5.3 Analysis of refraction seismic tomograms and quantification of velocity changes

5.3.1 Lapires

The results of the tomographic inversion of both data sets are shown in Fig. 8a (upper panels). To evaluate the RSTM approach in relation to the ERTM results, the corresponding ERT data sets are shown in the lower panels.

As the investigation depth of a refraction seismic survey depends not only on the survey geometry (source-receiver locations) but also on the characteristics of the subsurface layers, the investigation depth at ice-rich permafrost sites is often limited by the presence of a sharp refractor caused by the transition from the unfrozen active layer to the permafrost table. The amount of energy reflected/refracted to the surface is a function of the velocity contrast at an interface, with high velocity contrasts causing greater fractions of energy to be reflected or refracted to the surface (Burger et al., 2006). By this, the potential to resolve additional refractors at greater depth (e.g. the bedrock interface) decreases substantially. The refraction seismic tomograms in Fig. 8a illustrate this problem: the investigation depth is relatively shallow and does not exceed 15 m on average. Note, that the inversion scheme extrapolates calculated velocities, which are not covered by rays, from the given velocities of neighbouring cells into deeper areas (Sandmeier, 2008), as can be seen by the diagonal structures at greater depth (the maximum depth of penetration is marked by a dashed line).

The two tomograms from July and August are largely comparable concerning the overall structure, but exhibit different investigation depths and a clear shift in the transition between the low velocity overburden (red colours) and the material indicated by blue colours, corresponding to zone C in Fig. 4a, which is interpreted as the zone containing ground ice.

To quantitatively analyse the change in P-wave velocities from July to August, the velocity difference is displayed in terms of absolute velocities (m/s) and percentage change in Fig. 8b (upper panels). Additionally, the percentage resistivity change is

plotted for comparison (lower panel). For the interpretation of velocity changes the comparison must be restricted to those parts resolved by both data sets, that is the penetration depth in the earlier measurement in July 2008, indicated in Fig. 8b.

The velocity changes derived from independent tomographic inversion of both data sets largely correspond to the observations made from the analysis of travel time differences. As mentioned earlier, a velocity change may, strictly speaking, be solely a consequence of altered material characteristics, independently from a change in the depth of a refractor. Conversely, a shift in refractor depth (here due to the advance of the thawing front to greater depth) does not necessarily change the mean velocity of the respective layers, but the zone affected by this phase change obviously exhibits a velocity decrease (red colours) by the transition from one state (frozen) to the other (unfrozen), or vice versa (blue colours). Consequently, a thorough interpretation of the velocity change in terms of altered conditions within a layer, or change of refractor depth is only possible with respect to the absolute velocities in the refraction seismic tomograms.

The average negative velocity changes calculated from the tomograms are on the order of 20% to >50%, showing that the relatively small increase in travel times from July to August (on average by 2–15% with a maximum around 5%) represents a substantial change in subsurface characteristics.

5.3.2 Schilthorn

The results of tomographic inversion of the Schilthorn data sets are shown in Fig. 9 (upper panels) together with the corresponding ERT tomograms from the same date (lower panels). The quantification of the velocity differences in terms of absolute and percentage changes is illustrated in Fig. 10. In addition to the data discussed in detail in the previous sections, a third data set from a measurement in August 2009 is plotted here to show the potential application of a time-lapse refraction seismic approach in the context of operational annual permafrost monitoring. Similar to the Lapires site, a direct comparison is only possible for the depth range resolved in all tomograms restricting

the analysis to the uppermost three meters for comparisons with July 2008 (dashed lines in Figs. 9 and 10).

Despite the shallow zone suitable for a quantitative comparison, there are some common features in the uppermost three meters of all three tomograms. The tomogram from July shows a shallow refractor (v_p=4000–5000 m/s) at about 2 m depth but with distinct undulations: around 1015 m, between 1025 and 1035 m, and around 1040 m horizontal distance. Accordingly, the tomograms from August 2008 and 2009, with generally lower velocities, show small high-velocity anomalies (ca. 3500 m/s) around 1030 m and 1040 m horizontal distance that are slightly deeper. Conversely, no comparable feature is visible around 1015 m. The two tomograms from August 2008 and 2009 reveal a largely comparable structure and investigation depth, but with decreased velocities in 2009 below ca. 5 m depth.

5.4 Reliability

The reliability of the seismic tomograms can be judged qualitatively on the basis of the ray distributions, where synthetic ray paths are reconstructed by forward modelling based on the final model of the tomographic inversion. In general, large numbers of crossing rays indicate that velocities are well constrained by the travel time data, while regions not being sampled by rays indicate low confidence in the velocity estimates (Lanz et al., 1998). The results from network ray tracing (Sandmeier, 2008) for the data sets from both test sites are shown in Figs. 11 (Lapires) and 12 (Schilthorn). Note, that for better visibility of the velocity distribution only 25% of the calculated ray paths are plotted. Ray coverage, and therefore confidence in the velocity estimates, is generally high, but is reduced below ca. 20 m depth at Lapires and below 2.5 m depth in July and below 9 m in August at Schilthorn. Velocities determined at the base of the lowermost ray paths likely represent average values for the deep regions traversed (Musil et al., 2002), meaning that the confidence of these velocities is limited.

Quantitative measures to evaluate the reliability of the final tomograms are provided by REFLEXW by the *total absolute time difference* and the *total time difference* be-

tween the observed and calculated travel times. The total absolute time difference defines the sum of the absolute time differences independent from the sign (positive or negative difference) and gives an estimate on the overall adaptation of the tomogram. Conversely, the total time difference takes into account the sign of the differences and gives an estimate whether the mean model leads to too small or too large travel times, i.e. an interface is too shallow or too deep (Sandmeier, 2008).

The *total absolute time difference* between observed and calculated travel times amounts to 2.64 and 2.71 ms for July and August, respectively at Lapires, and to 0.46, 0.71 and 0.72 ms at Schilthorn. The generally higher values at Lapires are a function of the greater investigation depth and the resulting longer travel times. Whereas this value is well below the observed temporal shift in travel times at Schilthorn, demonstrating that the observed changes are significantly higher than the uncertainty of the inversion, the overall uncertainty of adaptation is on the same order of magnitude as the observed temporal shift in travel times in Lapires.

The *total time difference* between observed and calculated travel times amounts to 2.32 and 2.31 ms at Lapires, and to 0.03, −0.002 and −0.01 ms at Schilthorn for July 2008, August 2008, August 2009, meaning that the modelled data slightly underestimate the depth of the real structure in Lapires (i.e. observed – calculated travel times=positive values). At Schilthorn the very low values prove a high confidence in the depth of the modelled structures. As these values for the July and August measurements are very similar at both sites, respectively, the quality of adaptation can be considered equally well.

To further analyse the reliability of the observed velocity changes at Lapires, the differences between the travel times calculated by forward modelling from the tomographic inversion models of both measurement dates are plotted in Fig. 13 (equivalent to Fig. 5). Similar to the observed travel times, the calculated travel times show a temporal shift in measured travel times from July to August on the order of 1–4 ms (cf. Fig. 13b). This indicates that the overall misfit between model and data (total absolute time difference) of 2.64 and 2.71 ms does not seriously affect the accuracy of the de-

tection of changes in travel times. Rather do calculated and observed data correspond surprisingly well and demonstrate that the results from the travel time analysis are in good accordance with the results from the tomographic inversion.

6 Interpretation

As both the qualitative and quantitative analysis of the travel times and tomograms revealed a good reliability of the data sets, the tomograms and velocity changes are now interpreted for both sites.

6.1 Lapires

Comparing the seismic data with the ERT tomograms in Fig. 8a the results show good agreement and the subsurface structure derived from both methods can be summarised as follows:

- The active layer is characterised by low seismic velocities (due to high amounts of air in the voids between the unconsolidated blocks and fines) and intermediate resistivities (also caused by high amounts of air within the otherwise relatively conductive overburden).
- The left side of the profile represents the host material of the talus slope (unconsolidated blocks and fines) with low seismic velocities and comparatively low electrical resistivities. The investigation depth is insufficient to detect the depth of the underlying bedrock (>40 m).
- The high velocity and high resistivity anomaly within the central and right part of the tomograms delineate the presence of ice-rich permafrost. The observed average velocity of 3500 m/s could also indicate bedrock, but ground truth observations from an excavation (Delaloye et al., 2001), borehole data and ERT data (Delaloye, 2004; Hilbich, 2009), all indicate the presence of significant amounts

of ground ice, and no bedrock was encountered in all boreholes at this site (max. depth 40 m, personal communication Reynald Delaloye and Cristian Scapozza, 2008).

Regarding the comparatively large geophone spacing of 8 m (compared to 4 m electrode spacing), the resolution provided by the RST data sets is remarkable, which strikingly demonstrates the high potential of the RST method to resolve small-scale changes.

Regarding the time-lapse tomograms in Fig. 8b, the overall trend in velocity shift is negative, i.e. velocities generally decreased from July to August. However, large parts of the tomogram (at the surface and in the left (non-permafrost) part of the profile) exhibit only very small or even no changes in P-wave velocity. According to the above stated hypothesis, no considerable change in the content of frozen or liquid water has occurred in these zones and the general conditions did not change during the 40 days between the two measurements. These observations are consistent with borehole temperatures, which confirm already unfrozen conditions in the uppermost 2.5 m (or even more) in July. Also, the absence of pronounced changes in the unfrozen left part of the profile corresponds to the assumption that (from a geophysical point of view) seasonal changes at depth are much smaller in unfrozen regions than under permafrost conditions, as no phase changes between frozen and unfrozen conditions occur.

The red zones in Fig. 8b vividly illustrate the advance of the thawing front within the active layer during summer and indicate a reduction in P-wave velocity due to the melting of (seasonal) ground ice. The respective thaw depths (indicated in Fig. 8) are in good accordance with the resistivity changes (lower panel in Fig. 8b), and are generally above the zone of main observed velocity changes (upper panels). This suggests that the seismic signal is more sensitive to changes occurring below 0 °C, where the amount of unfrozen water already considerably increases with rising temperatures.

The only zone with a significant velocity increase (blue colours in Fig. 8b) is observed in the central part of the tomogram. A temporally increased velocity can be attributed

to either an increased water saturation compared to formerly lower water contents within unconsolidated sediments (Burger et al., 2006), or to the formation of ice (see Sect. 2). Both, ERT data from the same profile with high electric resistivities (indicative for ground ice), and permanently negative subsurface temperatures from nearby boreholes make the presence of large amounts of unfrozen water very unlikely (Hilbich, 2009). The latter hypothesis was already proposed from the analysis of ERT monitoring data (Hilbich, 2009). As seismic monitoring yields comparable results (Fig. 8b) this previous interpretation of ice formation from the ERTM results is now strikingly supported.

6.2 Schilthorn

Comparing the RST and ERT tomograms from the Schilthorn site (Fig. 9), the velocity and resistivity distributions exhibit clear differences (due to their complementary sensitivity to the physical properties of the subsurface). Regarding the overall temporal change visible in the time-lapse tomograms in Fig. 10, velocity changes correspond remarkably well to resistivity changes.

The interpretation of RST results from Schilthorn supported by the ERT results (Fig. 9) is summarised as follows:

- In July 2008 small parts of the profile were still covered by snow and the surface was very wet as a consequence of snow melt water that could not infiltrate into the still widely frozen ground. Active layer thickness was ca. 1.4 m and ca. 0.2 m in the two boreholes within the profile (Fig. 9). The shallow low velocity layer is interpreted as the active layer with a heterogeneous thickness, which is in agreement with the borehole data. The velocity of the refractor of 4000–5000 m/s is indicative of frozen conditions and/or bedrock. Due to the strong refractor and its relatively high velocities the investigation depth is limited, and no stratigraphic details can be resolved below ca. 2.5 m.
- At the end of August 2008 the snow has disappeared completely and surface

conditions were relatively dry. Active layer thickness has increased by up to 3 m (Fig. 9) within 47 days, which is clearly visible by the increased thickness of the red coloured zone indicating the active layer. The investigation depth increased to about 10 m with velocities of about 5000 m/s at the bottom. Velocities of 3000–4500 m/s in the lower part of the profile (between the permafrost table at about 5 m and the bottom) correspond to the frozen conditions recorded within the boreholes. The more heterogeneous velocity distribution in this layer may be attributed to a heterogeneous distribution of frozen debris and frozen bedrock. As velocities further increase to about 5000 m/s at greater depth it is assumed that the seismic velocity also represents transitions between weathered and firm bedrock.

– The increase in penetration depth is larger at the left side of the profile, which is in accordance to the ERT data that generally exhibit lower resistivities in this part, indicating the presence of debris compared to prevailing bedrock in the right part (see Hilbich et al., 2008).

In the time-lapse tomograms in Fig. 10 an overall velocity decrease is observed throughout the profile (above the dashed line) between July and August 2008. A very shallow zone at the surface (ca. 0.5 m) shows no change or partly a slight velocity increase, which can be explained by the initially unfrozen conditions with different degrees of saturation that may change depending on weather conditions or water supply from above. Below this superficial layer the P-wave velocity decreased by more than 3000 m/s, which is >75% of the absolute velocity. As major changes in the lithology and porosity can be excluded, this value cannot (only) be explained by seasonal variations in the air and/or water content but clearly indicates that the change in subsurface composition must have involved a significant amount of (seasonal) ground ice in the active layer, i.e. a change from primarily solid matrix conditions (rock-ice matrix) to a solid-liquid or a solid-liquid-gaseous matrix. As indicated by Eqs. (1) and (2) a comparable order of magnitude could only be achieved by significant changes in the pore volume with time and thus by variations in the air content (which is very unlikely within

the observed time span). The hypothesis of melting of ground ice is strongly supported by the borehole temperatures, that change from frozen to unfrozen conditions in the depth range of maximum velocity change (see thaw depths indicated at the boreholes in Figs. 10 and 14).

Whereas the absolute change in velocity between July and August 2008 is nearly uniformly distributed along the profile, the relative change is slightly increased in the left part of the profile (around 1005 m and 1015 m horizontal distance), indicating that the pore space and/or the ice content is higher than in the right part. This is in accordance with the findings by Hauck (2001) (based on a RST profile with larger penetration depth) as well as the interpretation of the ERT data (see Hilbich et al., 2008), which are considered to represent a several meters thick debris cover in the left part and bedrock with lower porosity in the right part. The resistivity changes observed by ERTM agree well with the seismic data set. Both methods reveal the lowest changes at the right end of the profile where bedrock outcrops indicate the occurrence of the bedrock layer close to the surface.

Comparing the data from August 2008 and August 2009, the common penetration depth is much deeper, allowing insights even below the permafrost table. Differences are small within the active layer, whose thickness is almost equal for 25 August 2008 (ca. 4.5 m) and 23 August 2009 (ca. 4.2 m), but a significant velocity decrease is observed below ca. 4 m during this one-year period. Borehole temperatures are consistent with this observation and confirm warmer permafrost conditions in 2009, which is mainly due to early snow fall in winter 2008/09 preventing the ground from effective cooling (Fig. 14). As for the Lapires site, this demonstrates the high sensitivity of the seismic signal to small changes in the unfrozen water content below the freezing point and thus the high potential of RSTM to detect permafrost degradation.

7 Conclusions

The novel refraction seismic tomography monitoring (RSTM) application presented in this paper is based on the assumption that P-wave velocities within the subsurface are affected by seasonal or inter-annual freezing or thawing processes, and that repeated refraction seismic measurements under constant measurement conditions allow the assessment of such temporal changes. The evaluation strategy of this approach comprised:

a) the analysis of reproducibility of the seismic signal,

b) the analysis of time-lapse travel time curves with respect to resolving possible shifts in travel times,

c) and the comparison of inverted tomograms including the quantification of spatio-temporal velocity changes.

Time-lapse data sets from the Lapires talus slope and the Schilthorn rock slope served to evaluate the performance of the RSTM approach. Both sites are characterised by pronounced differences in the seasonal changes during the same period. For Schilthorn, an additional data set after one year allowed a comparison on an annual time scale. Important results from this study are summarised in the following:

– Waveforms and signal strength revealed a generally good reproducibility for subsequent measurements with moderate changes in active layer depth (as observed at Lapires).

– The observed travel times of the repeated measurements showed systematic spatio-temporal changes.

– Tomographic inversion results are largely comparable concerning the overall structure, but exhibit different investigation depths and a clear shift in the transition between the low velocity overburden and the refractor underneath.

– The temporal shift is well reconstructed in the calculated travel times from the inverted models (by forward modelling) indicating that the overall misfit between model and observed data does not seriously affect the accuracy of the detection of travel time changes.

– The interpretation of velocity changes from time-lapse tomograms corresponds to the results from ERT monitoring, and to the thawing front progression. No significant changes were observed in initially already unfrozen parts of the active layer.

– An important result is, that the observed velocity change of ~3000 m/s at the Schilthorn site unambiguously proved the initial presence of significant amounts of ground ice in the active layer, which disappeared until the date of the later measurement. This is a great advantage of the RSTM approach compared to ERTM, and RSTM therefore provides a huge potential to avoid ambiguities regarding the detection of permafrost degradation.

– Another advantage of the RSTM approach is the generally higher vertical resolution than that revealed by ERT surveys, even for a geophone spacing larger than the corresponding electrode spacing. Together with the high reproducibility of the seismic signal in case of relatively small changes this points to a remarkable potential to resolve anticipated smaller-scale changes in ground ice content for inter-annual comparisons.

– A serious limitation of the approach is the often small penetration depth due to strong velocity contrasts between active layer and permafrost table. Moreover, as the acquisition of high-resolution data sets cannot easily be automated and data processing is based on manual picking of first arrivals, the overall efforts of RSTM are much higher than for ERTM. However, the acquisition of at least one data set in late summer per site and per year is sufficient for a long-term analysis of climate related ground ice degradation, and is feasible with a reasonable effort.

The time-lapse seismic refraction approach provides a valuable potential in terms of an independent and complementary monitoring approach for the detection of altered subsurface conditions caused by freezing and thawing processes. The approach was evaluated on a seasonal time scale, but its general applicability to annual changes could be shown for one example from Schilthorn. As inter-annual changes in response to global warming are believed to be on a similar order of magnitude as seasonal changes, RSTM will work equally well on longer time scales and will be applied to those within the next years.

Acknowledgements. The author thanks Damien Abbet, Jonathan Dorthe, Tobias Hördt, and Christian Hauck for motivated help during data acquisition, and Christian Hauck and Reynald Delaloye for detailed discussions of the data. The borehole temperatures were kindly provided by PERMOS. The generous logistical support from the Schilthornbahn AG is also acknowledged. The study was financed by the German Research Foundation DFG (MA1308_22-1).

References

Burger, H. R., Sheehan, A. F., and Jones, C. H.: Introduction to Applied Geophysics – Exploring the Shallow Subsurface, W. W. Norton and Company, Inc., London, 554 pp., 2006.

Delaloye, R.: Contribution à l'étude du pergélisol de montagne en zone marginale, Ph.D. thesis, Département de Géosciences – Géographie, Fribourg, University of Fribourg, 242 pp., 2004.

Delaloye, R. and Lambiel, C.: Evidences of winter ascending air circulation throughout talus slopes and rock glaciers situated in the lower belt of alpine discontinuous permafrost (Swiss Alps), Norsk Geogr. Tidsskr., 59(2), 194–203, 2005.

Delaloye, R., Reynard, E., and Lambiel, C.: Pergélisol et construction de remontées mécaniques: l'exemple des Lapires (Mont-Gelé, Valais), Le gel en géotechnique, Publications de la Société Suisse de Mécanique des Sols et des Roches, 141, 103–113, 2001.

Fortier, R., Allard, M., and Seguin, M. K.: Effect of physical-properties of frozen ground on electrical-resistivity logging, Cold. Reg. Sci. Technol., 22(4), 361–384, 1994.

Harris, C., Arenson, L. U., Christiansen, H. H., Etzelmüller, B., Frauenfelder, R., Gruber, S., Haeberli, W., Hauck, C., Hoelzle, M., Humlum, O., Isaksen, K., Kääb, A., Kern-

Lütschg, M. A., Lehning, M., Matsuoka, N., Murton, J. B., Noetzli, J., Phillips, M., Ross, N., Seppälä, M., Springman, S., and Vonder Mühll, D.: Permafrost and climate in Europe: Monitoring and modelling thermal, geomorphological and geotechnical responses, Earth-Sci. Rev., 92, 117–171, 2009.

Harris, C. and Cook, J. D.: The detection of high altitude permafrost in Jotunheimen, Norway using seismic refraction techniques: An assessment, Arctic Alpine Res., 18(1), 19–26, 1986.

Harris, C. and Isaksen, K.: Recent warming of European permafrost: Evidence from borehole monitoring, in: Proceedings of the 9th International Conference on Permafrost, Fairbanks, Alaska, 1, 655–661, 2008.

Harris, C., Vonder Mühll, D., Isaksen, K., Haeberli, W., Sollid, J. L., King, L., Holmlund, P., Dramis, F., Guglielmin, M., and Palacios, D.: Warming permafrost in European mountains, Global Planet. Change, 39(3–4), 215–225, 2003.

Hauck, C.: Geophysical methods for detecting permafrost in high mountains, Ph.D. thesis, Mitteilungen der Versuchsanstalt für Wasserbau, Hydrologie und Glaziologie der Eidgenössischen Technischen Hochschule Zürich, Nr. 171, ETH Zürich, 204 pp., 2001.

Hauck, C.: Frozen ground monitoring using DC resistivity tomography, Geophys. Res. Lett., 29(21), 2016, doi:10.1029/2002GL014995, 2002.

Hauck, C., Bach, M., and Hilbich, C.: A 4-phase model to quantify subsurface ice and water content in permafrost regions based on geophysical data sets, in: Proceedings of the 9th International Conference on Permafrost, Fairbanks, Alaska, 1, 675–680, 2008.

Hauck, C., Isaksen, K., Mühll, D. V., and Sollid, J. L.: Geophysical surveys designed to delineate the altitudinal limit of mountain permafrost: an example from Jotunheimen, Norway, Permafrost Periglac., 15(3), 191–205, 2004.

Hauck, C. and Vonder Mühll, D.: Evaluation of geophysical techniques for application in mountain permafrost studies, Z. Geomorphol. Supp., 132, 159–188, 2003.

Hausmann, H., Krainer, K., Brückl, E., and Mostler, W.: Internal structure and ice content of Reichenkar rock glacier (Stubai Alps, Austria) assessed by geophysical investigations, Permafrost Periglac., 18(4), 351–367, 2007.

Hilbich, C.: Geophysical monitoring systems to assess and quantify ground ice evolution in mountain permafrost, Ph.D. thesis, Department of Geography, University of Jena, 173 pp., online available at: http://www.db-thueringen.de/servlets/DocumentServlet?id=13905, 2009.

Hilbich, C., Hauck, C., Hoelzle, M., Scherler, M., Schudel, L., Völksch, I., Vonder Mühll, D.,

and Mäusbacher, R.: Monitoring mountain permafrost evolution using electrical resistivity tomography: A 7-year study of seasonal, annual, and long-term variations at Schilthorn, Swiss Alps, J. Geophys. Res., 113, F01S90, doi:10.1029/2007JF000799, 2008.
Ikeda, A.: Combination of conventional geophysical methods for sounding the composition of rock glaciers in the Swiss Alps, Permafrost Periglac., 17(1), 35–48, 2006.
Imhof, M., Pierrehumbert, G., Haeberli, W., and Kienholz, H.: Permafrost investigation in the Schilthorn massif, Bernese Alps, Switzerland, Permafrost Periglac., 11, 189–206, 2000.
King, M. S.: Rock-physics developments in seismic exploration: a personal 50-year perspective, Geophysics, 70(6), 3–8, 2005.
Kneisel, C., Hauck, C., Fortier, R., and Moorman, B.: Advances in geophysical methods for permafrost investigations, Permafrost Periglac., 19(2), 157–178, 2008.
Lambiel, C.: Inventaire des glaciers rocheux entre la Val de Bages et le Val d'Hérémence (Valais), Ph.D. thesis, University of Lausanne, 167 pp., 1999.
Landrø, M., Nguyen, A. K., and Mehdizadeh, H.: Time lapse refraction seismic – a tool for monitoring carbonate fields?, in: SEG International Exposition and 74th Annual Meeting, 10–15 October 2004, Denver, Colorado, 1–4, 2004.
Lanz, E., Maurer, H., and Green, A. G.: Refraction tomography over a buried waste disposal site, Geophysics, 63(4), 1414–1433, 1998.
Maurer, H. and Hauck, C.: Geophysical imaging of alpine rock glaciers, J. Glaciol., 53(180), 110–120, 2007.
Musil, M., Maurer, H., Green, A. G., Horstmeyer, H., Nitsche, F. O., Vonder Mühll, D., and Springman, S.: Shallow seismic surveying of an Alpine rock glacier, Geophysics, 67(6), 1701–1710, 2002.
PERMOS: Permafrost in Switzerland 2004/2005 and 2005/2006, in: Glaciological Report (Permafrost) No. 6/7 of the Cryospheric Commission (CC) of the Swiss Academy of Sciences (SCNAT) and the Department of Geography, edited by: Noetzli, J., Naegeli, B., and Vonder Mühll, D., University of Zurich, 61 pp., 2009.
Reynolds, J. M.: An Introduction to Applied and Environmental Geophysics, Wiley, Chichester, 796 pp., 1997.
Röthlisberger, H.: Seismic Exploration in Cold Regions, Cold Regions Research and Engineering Laboratory, Hanover, 139 pp., 1972.
Sandmeier, K. J.: REFLEXW – Windows™ 9x/NT/2000/XP-program for the processing of seismic, acoustic or electromagnetic reflection, refraction and transmission data, 2008.

Scott, W. J., Sellmann, P. V., and Hunter, J. A.: Geophysics in the study of permafrost, in: Geotechnical and Environmental Geophysics, edited by: Ward, S., Society of Exploration Geophysics, Tulsa, 355–384, 1990.

Timur, A.: Velocity of compressional waves in porous media at permafrost temperatures, Geophysics, 33(4), 584–595, 1968.

Vesnaver, A. L., Accainoz, F., Bohmz, G., Madrussaniz, G., Pajchel, J., Rossiz, G., and Dal Moro, G.: Time-lapse tomography, Geophysics, 68(3), 815–823, 2003.

Vonder Mühll, D., Noetzli, J., Roer, I., Makowski, K., and Delaloye, R.: Permafrost in Switzerland 2002/2003 and 2003/2004, Glaciological Report (Permafrost) No. 4/5 of the Cryospheric Commission (CC) of the Swiss Academy of Sciences (SCNAT) and the Department of Geography, University of Zurich, 106, 2007.

Vonder Mühll, D. S.: Geophysikalische Untersuchungen im Permafrost des Oberengadins, Ph.D. thesis, ETH Zürich, Diss. ETH Nr. 10107, 222 pp., 1993.

Wyllie, M. R. J., Gregory, A. R., and Gardner, L. W.: Elastic wave velocities in heterogeneous and porous media, Geophysics, XXI(1), 41–70, 1956.

Zimmerman, R. W. and King, M. S.: The effect of the extent of freezing on seismic velocities in unconsolidated permafrost, Geophysics, 51(6), 1285–1290, 1986.

Table 1. Measurement details for the seismic monitoring test sites (abbreviations: AL=active layer thickness, n.a.=not available).

	Lapires	Schilthorn
dates of measurement (respective active layer depths in boreholes)	10 Jul 2008 (AL 4/2.5 m) 18 Aug 2008 (AL 5/5 m)	11 Jul 2008 (AL 1.4/0.2 m) 26 Aug 2008 (AL 4.5/1.5 m) 23 Aug 2009 (AL 4.2/n.a. m)
number of geophones	23	24
geophone spacing	8 m	2 m
profile length	176 m	46 m
number of shot points	24	24
off-end shots (distance from first/last geophone)	4/4 m	−/1 m

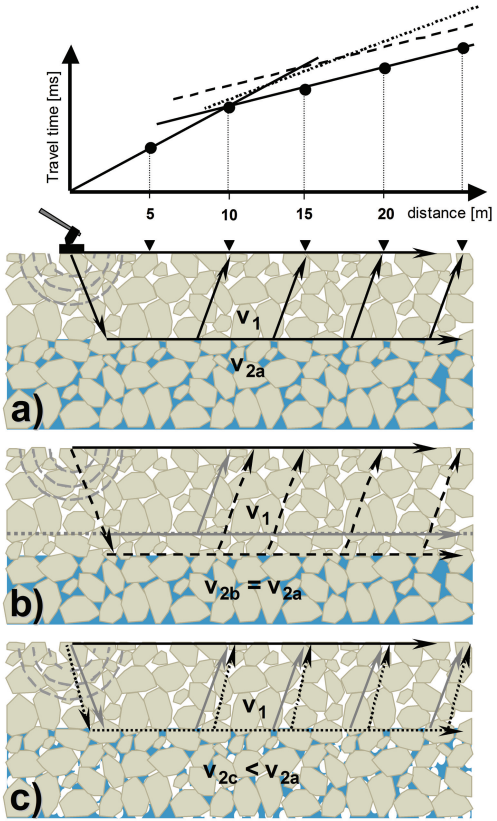

Fig. 1. Idealised principle of time-lapse refraction seismic based on **(a)** a two-layer subsurface model with a coarse-blocky unfrozen overburden with air-filled voids and a saturated rock-ice-matrix underneath. The lower panels illustrate the change of travel times as a consequence of **(b)** a vertical shift of the refractor (e.g. the seasonally varying interface between frozen and unfrozen conditions), and **(c)** altered ice (and air) contents within the lower layer causing changes in seismic velocity. The corresponding travel time curves for all three scenarios are given above.

TCD
4, 77–119, 2010

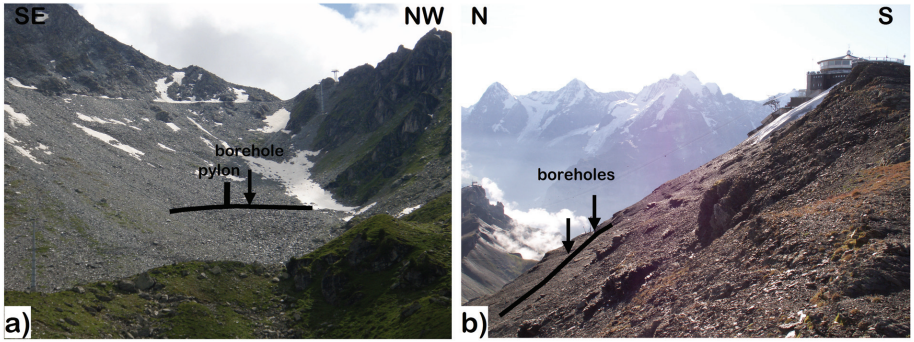

Fig. 2. Photographs of the test sites: **(a)** Lapires talus slope, and **(b)** the Schilthorn rock slope. The RST profile lines and the positions of the boreholes are highlighted.

TCD
4, 77–119, 2010

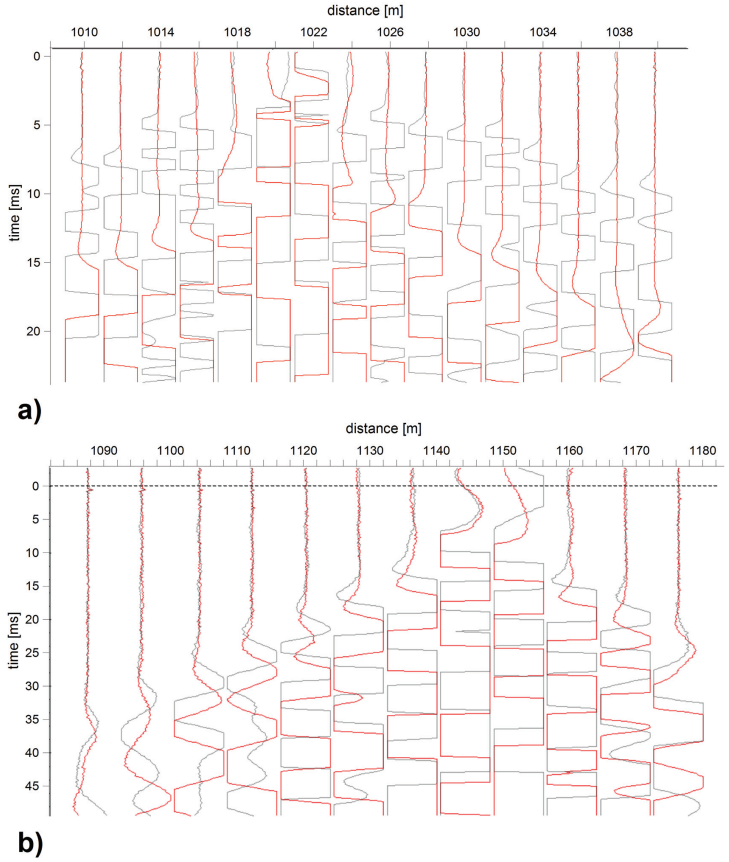

Fig. 3. Detailed view of a time-lapse seismogram from Lapires for the shot position at 1148 m with traces from 10 July (grey) and 18 August 2008 (red), and from Schilthorn at the shot position at 1021 m with traces from 11 July (grey) and 26 August 2008 (red). Note the time shifts of the first arrivals for the later date.

TCD
4, 77–119, 2010

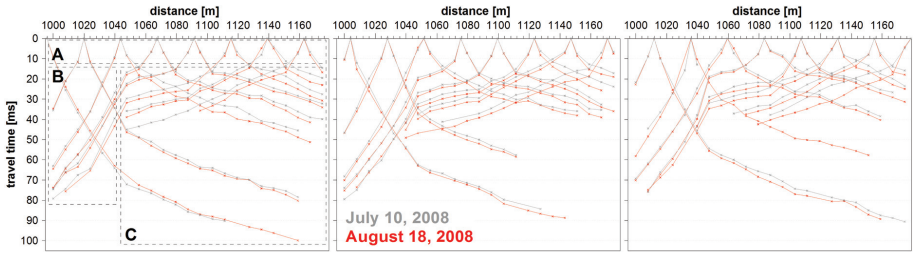

Fig. 4. Comparison of travel times from 10 July (grey) and 18 August 2008 (red), distributed into three separated plots for clarity. Note, that in some cases the absence of single picks may change the slope of the travel time curve.

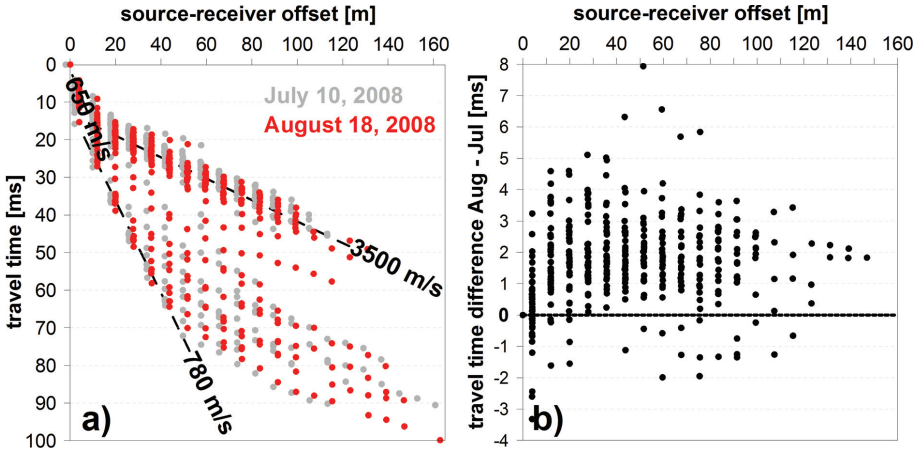

Fig. 5. **(a)** Travel times for 10 July 2008 (grey) and 18 August 2008 (red) (as in Fig. 4), but sorted by the absolute offset between geophone and shot point (for better visibility of both data sets the *x* axis was slightly shifted to the right for 10 July 2008). **(b)** Calculated travel time differences between August and July, sorted by source-receiver offset.

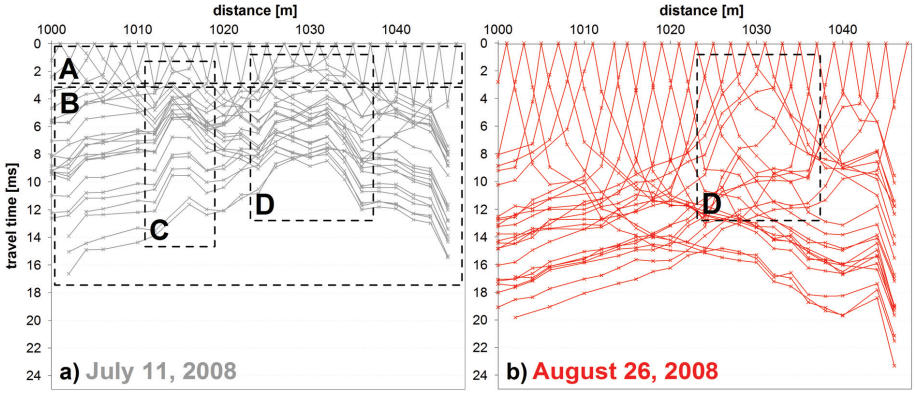

Fig. 6. Combined travel time curves for the measurement at Schilthorn from **(a)** 11 July 2008 (grey) and **(b)** 26 August 2008 (red).

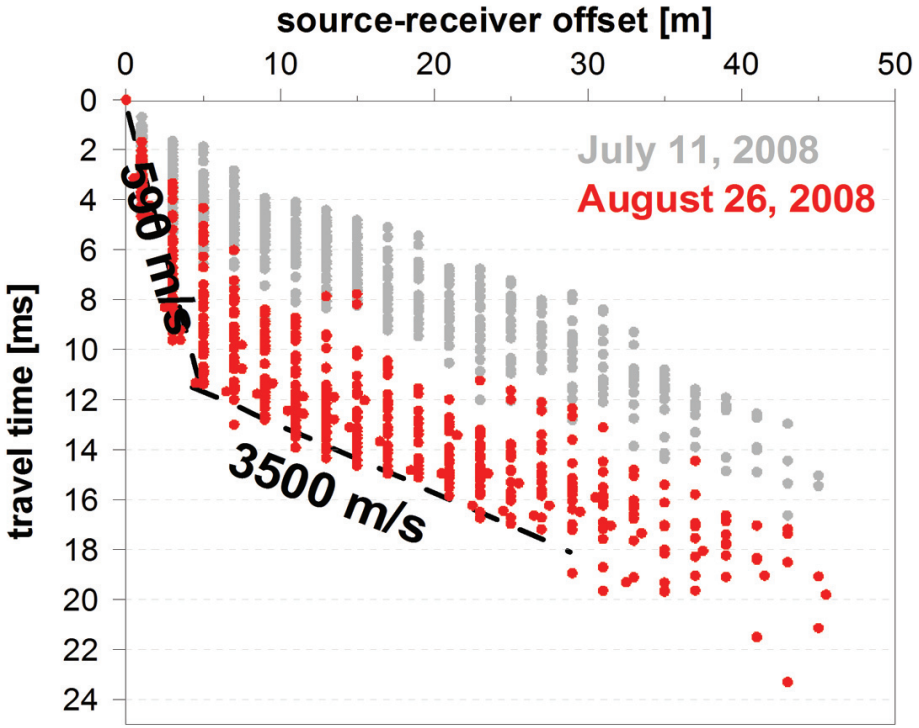

Fig. 7. Common offset plot of the travel times at Schilthorn for 11 July 2008 and 26 August 2008.

TCD
4, 77–119, 2010

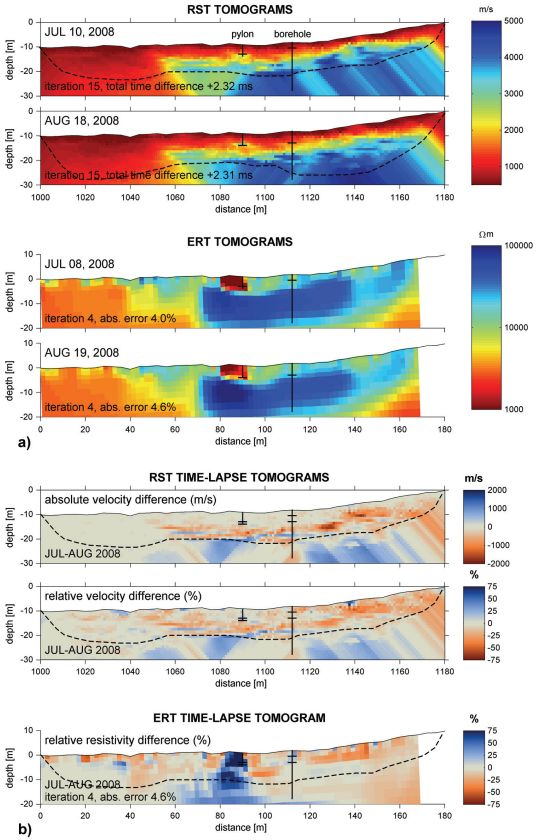

Fig. 8. **(a)** Comparison of RST tomograms from 10 July and 19 August 2008 at Lapires with ERT tomograms from comparable dates. **(b)** Comparison of temporal change in seismic velocities with resistivity changes. The resolved investigation depth is marked by a dashed line. Locations of the pylon and the borehole are indicated, as well as the respective active layer thickness at both positions (a), and for both dates in (b).

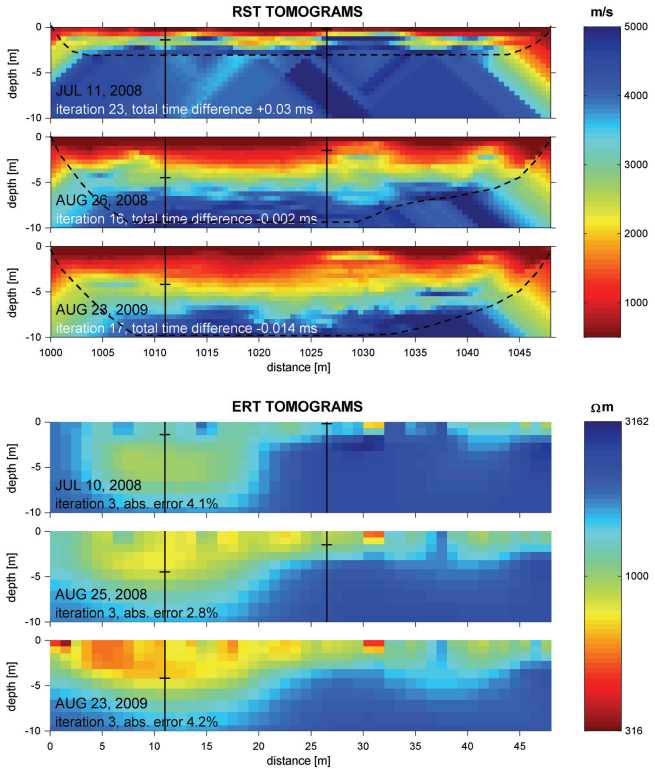

Fig. 9. Comparison of RST and ERT tomograms for July 2008, August 2008, and August 2009 at Schilthorn. The resolved investigation depth is marked with dashed lines. Locations of the boreholes and the respective active layer thickness are indicated.

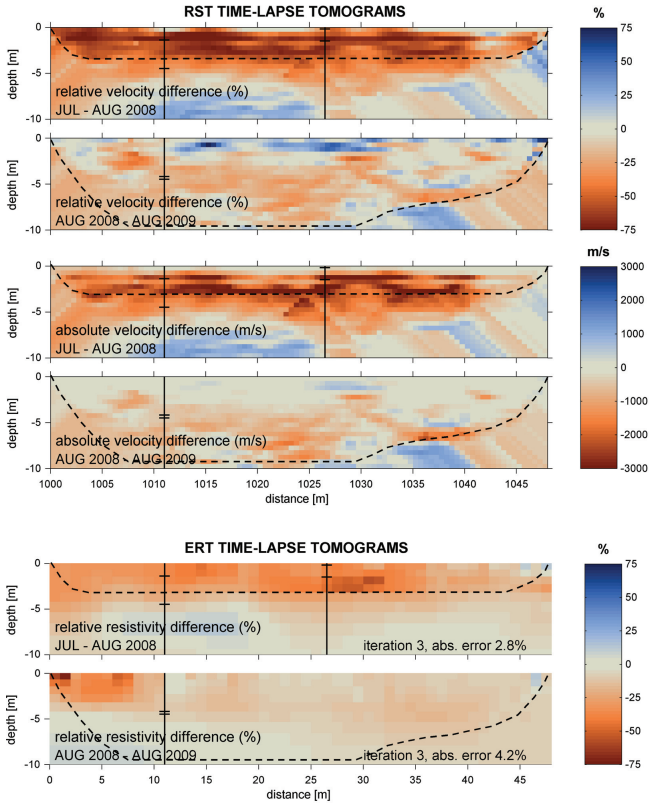

Fig. 10. Comparison of temporal change in seismic velocities with changes in electric resistivities for July to August 2008, and August 2008 to August 2009. The maximum common investigation depths are marked as the lower boundary for direct comparisons. Locations of the boreholes and the respective active layer thickness for both dates are indicated.

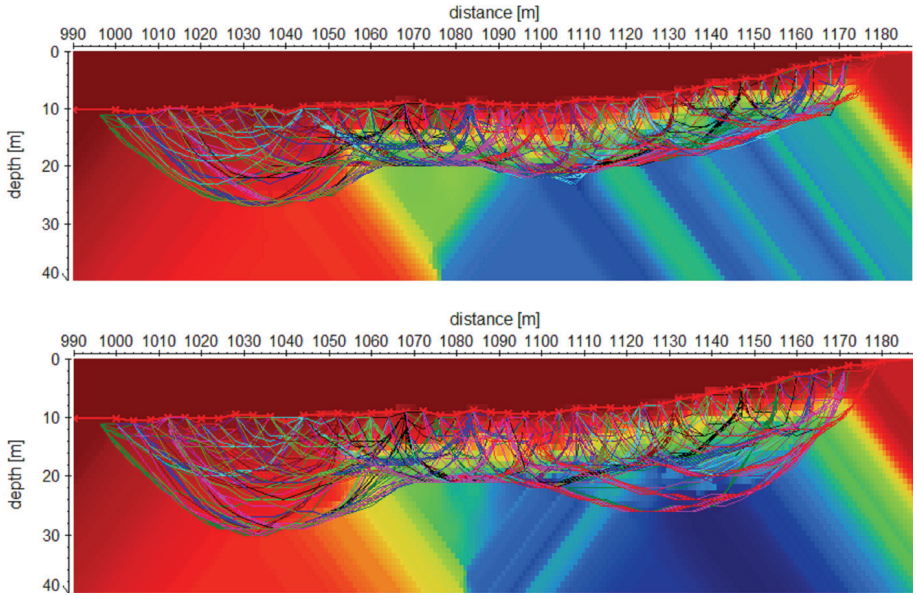

Fig. 11. Calculated ray paths for the tomograms from Lapires: 10 July 2008 (top), and 18 August 2008 (bottom).

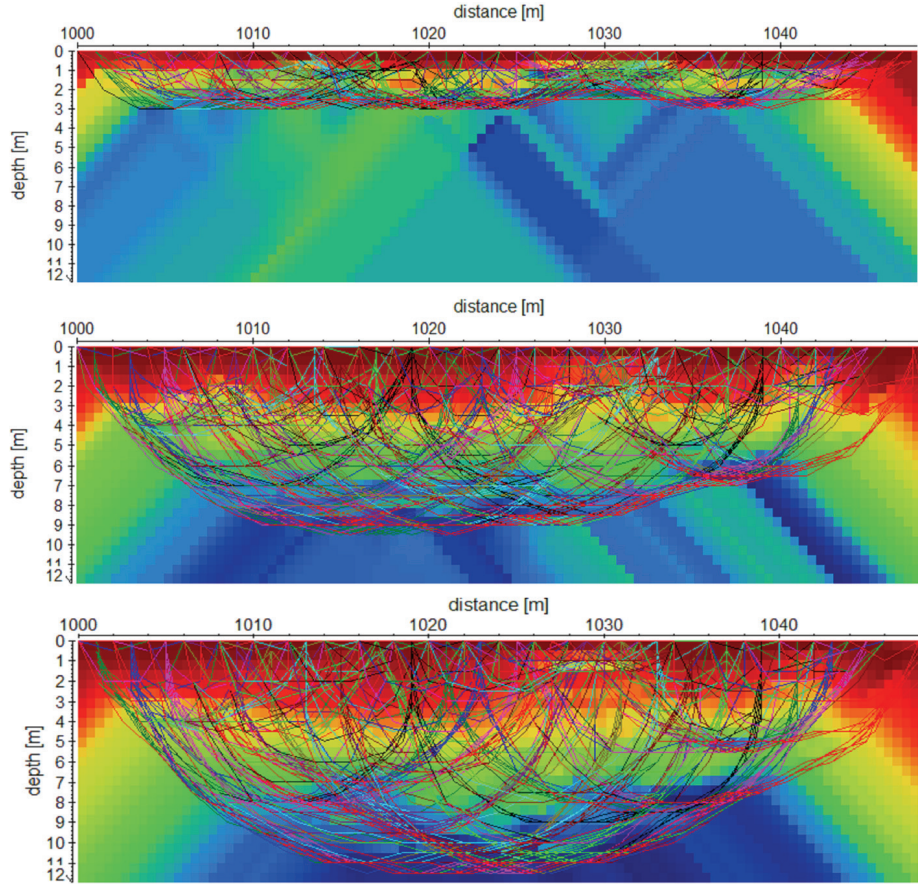

Fig. 12. Calculated ray paths for the tomograms from Schilthorn: 11 July 2008 (top), and 26 August 2008 (middle), and 23 August 2009 (bottom). Note that the depth scale is smaller than in Fig. 11.

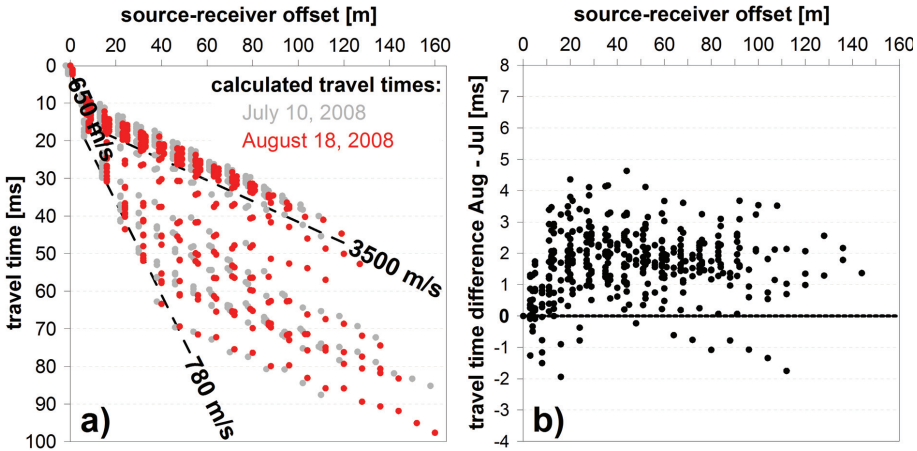

Fig. 13. As in Fig. 5, but now for **(a)** calculated travel times based on the tomographic inversion models displayed in Fig. 8a against source-receiver offset, **(b)** differences in calculated travel times against offset.

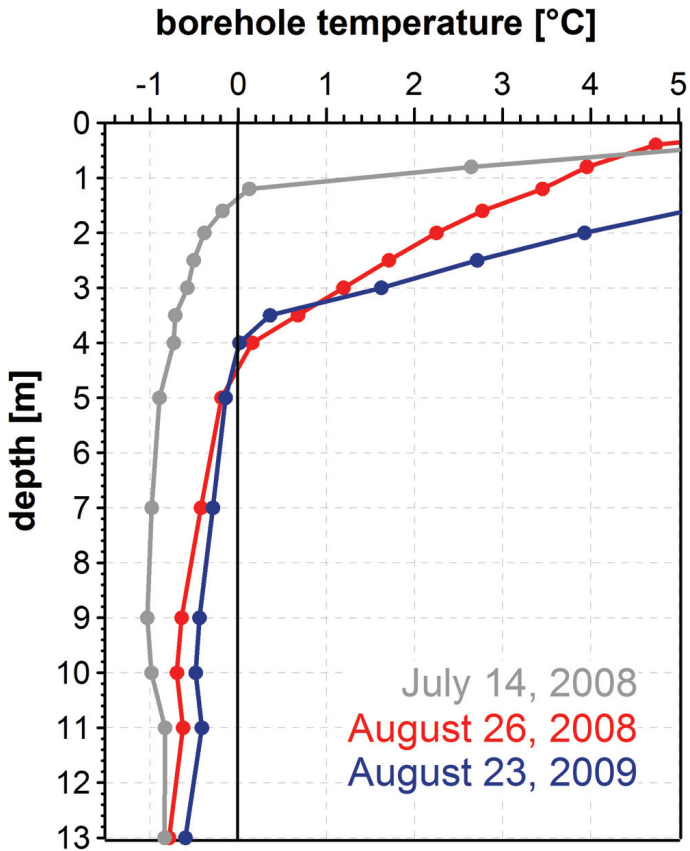

Fig. 14. Borehole temperatures for Schilthorn (left borehole in Figs. 9 and 10) at the measurement dates (data provided by PERMOS).